# Phase-field modelling of the coupled microstructure and fracture evolution in ferroelectric single crystals

Advanced Discretization Methods - Fall 2017

Saskia Loosveldt & Rafael Pacheco

# Introduction

- Wide use of ferroelectric ceramics due to their electromechanical coupling properties
- Inherently brittle
- Complex fracture processes due to the interaction between crack tip stress fields and formation of subdomains in the ferroelectric

- Aim of this work: analyze the quasi-static crack propagation and ferroelectric domain formation under combined electromechanical loads

# Introduction

- Coupled phase-field model to study brittle crack propagation and microstructure evolution
- Benefits
  - 1 PDE to simultaneously track interfaces and model interfacial phenomena
  - Variational formulation
- Drawbacks
  - High computational cost
- Interface or jump BC must be encoded into the phase field

# Phase field model of brittle fracture in ferroelectric materials

Ferroelectric single crystals

- Electromechanical enthalpy density derived from the Helmholtz free energy

$$\psi(\boldsymbol{\varepsilon}, \mathbf{p}, \nabla\mathbf{p}, \mathbf{D}) = U(\nabla\mathbf{p}) + W(\mathbf{p}, \boldsymbol{\varepsilon}) + \chi(\mathbf{p}) + \frac{1}{2\varepsilon_0}(\mathbf{D} - \mathbf{p}) \cdot (\mathbf{D} - \mathbf{p})$$

$$\begin{aligned} h(\boldsymbol{\varepsilon}, \mathbf{p}, \nabla\mathbf{p}, \mathbf{E}) &= \min_{\mathbf{D}} \left[\psi(\boldsymbol{\varepsilon}, \mathbf{p}, \nabla\mathbf{p}, \mathbf{D}) - \mathbf{E} \cdot \mathbf{D}\right] \\ &= U(\nabla\mathbf{p}) + W(\mathbf{p}, \boldsymbol{\varepsilon}) + \chi(\mathbf{p}) - \frac{\varepsilon_0}{2}|\mathbf{E}|^2 - \mathbf{E} \cdot \mathbf{p} \end{aligned}$$

# Phase field model of brittle fracture in ferroelectric materials

Ferroelectric single crystals

- $U(\nabla p)$, $W(p,\varepsilon)$ and $\chi(p)$ are energy functions assuming plane polarization/strain

$$U(p_{i,j}) = \frac{a_0}{2}(p_{1,1}^2 + p_{1,2}^2 + p_{2,1}^2 + p_{2,2}^2)$$

$$W(p_i, \varepsilon_{jk}) = -\frac{b_1}{2}(\varepsilon_{11}p_1^2 + \varepsilon_{22}p_2^2) - \frac{b_2}{2}(\varepsilon_{11}p_2^2 + \varepsilon_{22}p_1^2) - b_3(\varepsilon_{21} + \varepsilon_{12})p_1p_2 + \frac{c_1}{2}(\varepsilon_{11}^2 + \varepsilon_{22}^2) + c_2\varepsilon_{11}\varepsilon_{22} + \frac{c_3}{2}(\varepsilon_{12}^2 + \varepsilon_{21}^2),$$

$$\chi(p_i) = \alpha_1(p_1^2 + p_2^2) + \alpha_{11}(p_1^4 + p_2^4) + \alpha_{12}(p_1^2p_2^2) + \alpha_{111}(p_1^6 + p_2^6) + \alpha_{112}(p_1^2p_2^4 + p_2^2p_1^4) + \alpha_{1111}(p_1^8 + p_2^8) + \alpha_{1112}(p_1^6p_2^2 + p_2^6p_1^2) + \alpha_{1122}(p_1^4p_2^4),$$

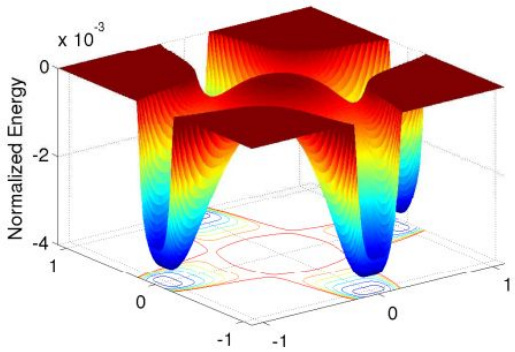

# Phase field model of brittle fracture in ferroelectric materials

Ferroelectric single crystals

- Total electromechanical enthalpy

$$H[\boldsymbol{u}, \mathbf{p}, \phi] = \int_{\Omega} h(\boldsymbol{\varepsilon}(\boldsymbol{u}), \mathbf{p}, \nabla \mathbf{p}, \mathbf{E}(\phi)) \mathrm{d}\Omega - \int_{\Gamma_{N,\boldsymbol{u}}} \boldsymbol{t} \cdot \boldsymbol{u} \, \mathrm{d}S + \int_{\Gamma_{N,\phi}} \omega\phi \, \mathrm{d}S$$

# Phase field model of brittle fracture in ferroelectric materials

Phase field model for brittle fracture

- Total energy of a body made of brittle material following regularized Griffith's fracture theory

$$E_\kappa[\boldsymbol{u}, v] = \int_\Omega (v^2 + \eta_\kappa) F(\boldsymbol{\varepsilon}(\boldsymbol{u}))\, \mathrm{d}\Omega + G_c \int_\Omega \left[ \frac{(1-v)^2}{4\kappa} + \kappa |\nabla v|^2 \right] \mathrm{d}\Omega - \int_{\Gamma_{N,\boldsymbol{u}}} \boldsymbol{t} \cdot \boldsymbol{u}\, \mathrm{d}S$$

# Phase field model of brittle fracture in ferroelectric materials

Brittle fracture in ferroelectric ceramics

- Coupling between crack phase field and other fields is determined by the electrical and mechanical BC
- Mechanical BC: traction-free crack faces

$\boldsymbol{\sigma} \cdot \boldsymbol{n} = 0$ → $(v^2 + \eta_\kappa)$ elastic energy *F* / electroelastic energy *W*

# Phase field model of brittle fracture in ferroelectric materials

Brittle fracture in ferroelectric ceramics

- Electrical BC: Permeable crack

$$\phi^+ = \phi^- \quad \text{and} \quad \mathbf{D}^+ \cdot \boldsymbol{n}^+ = \mathbf{D}^- \cdot \boldsymbol{n}^- \rightarrow$$

electric field *E* is not modified

- Electrical BC: Impermeable crack

$$\mathbf{D}^+ \cdot \boldsymbol{n}^+ = \mathbf{D}^- \cdot \boldsymbol{n}^- = 0 \rightarrow (v^2 + \eta_\kappa)$$

electric field *E*

- Electrical BC: Free polarization

$$\frac{d\mathrm{p}_i^+}{dn} = \frac{d\mathrm{p}_i^-}{dn} = 0, (i = 1, 2) \rightarrow (v^2 + \eta_\kappa)$$

domain wall energy *U*

# Phase field model of brittle fracture in ferroelectric materials

Brittle fracture in ferroelectric ceramics

- Enthalpy for a traction free, permeable and free polarization crack

$$h(\boldsymbol{\varepsilon}, \mathbf{p}, \nabla\mathbf{p}, \mathbf{E}, v) = (v^2 + \eta_\kappa)\,[U(\nabla\mathbf{p}) + W(\mathbf{p}, \boldsymbol{\varepsilon})] + \chi(\mathbf{p}) - \frac{\varepsilon_0}{2}|\mathbf{E}|^2 - \mathbf{E}\cdot\mathbf{p}$$

- Enthalpy for a traction free, impermeable and free polarization crack

$$h(\boldsymbol{\varepsilon}, \mathbf{p}, \nabla\mathbf{p}, \mathbf{E}, v) = (v^2 + \eta_\kappa)\left[U(\nabla\mathbf{p}) + W(\mathbf{p}, \boldsymbol{\varepsilon}) - \frac{\varepsilon_0}{2}|\mathbf{E}|^2 - \mathbf{E}\cdot\mathbf{p}\right] + \chi(\mathbf{p})$$

- Total electromechanical energy of a ferroelectric body

$$H[\boldsymbol{u}, v, \mathbf{p}, \phi] = \int_\Omega h(\boldsymbol{\varepsilon}(\boldsymbol{u}), \mathbf{p}, \nabla\mathbf{p}, \mathbf{E}(\phi), v)\ \mathrm{d}\Omega\ + G_c \int_\Omega \left[\frac{(1-v)^2}{4\kappa} + \kappa|\nabla v|^2\right]\ \mathrm{d}\Omega - \int_{\Gamma_{N,\boldsymbol{u}}} \boldsymbol{t}\cdot\boldsymbol{u}\ \mathrm{d}S + \int_{\Gamma_{N,\phi}} \omega\phi\ \mathrm{d}S$$

# Phase field model of brittle fracture in ferroelectric materials

Brittle fracture in ferroelectric ceramics

- Weak form + Electrostatic equilibrium

$$
\begin{aligned}
\mu_p \int_\Omega \dot{p}_i \delta p_i \, \mathrm{d}\Omega &= -\delta H[\boldsymbol{u}, v, \mathbf{p}, \phi; \delta \boldsymbol{p}] = -\int_\Omega \frac{\partial h}{\partial p_i} \delta p_i \, \mathrm{d}\Omega, \\
\mu_v \int_\Omega \dot{v} \delta v \, \mathrm{d}\Omega &= -\delta H[\boldsymbol{u}, v, \mathbf{p}, \phi; \delta v] \\
&= -\int_\Omega \frac{\partial h}{\partial v} \delta v \, \mathrm{d}\Omega - 2G_c \int_\Omega \left( \frac{v-1}{4\kappa} \delta v + \kappa v_{,i} \delta v_{,i} \right) \, \mathrm{d}\Omega, \\
0 &= \delta H[\boldsymbol{u}, v, \mathbf{p}, \phi; \delta \boldsymbol{u}] = \int_\Omega \frac{\partial h}{\partial \varepsilon_{ij}} \delta \varepsilon_{ij} \, \mathrm{d}\Omega - \int_{\Gamma_{N,u}} t_i \delta u_i \, \mathrm{d}S, \\
0 &= -\delta H[\boldsymbol{u}, v, \mathbf{p}, \phi; \delta \phi] = -\int_\Omega \frac{\partial h}{\partial E_i} \delta E_i \, \mathrm{d}\Omega - \int_{\Gamma_{N,\phi}} \omega \delta \phi \, \mathrm{d}S
\end{aligned}
$$

# Phase field model of brittle fracture in ferroelectric materials

Brittle fracture in ferroelectric ceramics

- FEM discretization + semi-implicit time discretization + staggered approach

**Algorithm 1** for the coupled model

Let $m = 0$
Set $v_0 = 1$, $\mathbf{p}_0 = \mathbf{p}_{init}$, $\phi_0 = 0$ and $\boldsymbol{u}_0 = 0$ if $n = 0$
Set $v_0 = v^{n-1}$, $\boldsymbol{u}_0 = \boldsymbol{u}^{n-1}$, $\mathbf{p}_0 = \mathbf{p}^{n-1}$ and $\phi_0 = \phi^{n-1}$ if $n > 0$
**repeat**
  $m \longleftarrow m + 1$
  Compute $\mathbf{p}_m$ in (15) using $\mathbf{p}_{m-1}$, $\boldsymbol{u}_{m-1}$, $\phi_{m-1}$ and $v_{m-1}$
  Compute $\boldsymbol{u}_m$ in (17) using $\mathbf{p}_m$ and $v_{m-1}$ under the constraint $\boldsymbol{u}_m = \boldsymbol{g}(t^n)$ on $\Gamma_{D,\boldsymbol{u}}$
  Compute $\phi_m$ in (18) using $\mathbf{p}_m$ and $v_{m-1}$ under the constraint $\phi_m = f(t^n)$ on $\Gamma_{D,\phi}$
  Compute $v_m$ in (16) using $\mathbf{p}_m$, $\boldsymbol{u}_m$, $\phi_m$ and $v_{m-1}$ under the constraint $v_m = 0$ for $v^{n-1} \leqslant \alpha$
**until** $\|\mathbf{p}_m - \mathbf{p}_{m-1}\|_\infty \leqslant \delta_{ferro}$ and $\|v_m - v_{m-1}\|_\infty \leqslant \delta_{vfield}$
Set $\boldsymbol{u}^n = \boldsymbol{u}_m$, $v^n = v_m$, $\mathbf{p}^n = \mathbf{p}_m$ and $\phi^n = \phi_m$

# Numerical simulations

Computational domain and parameter setting

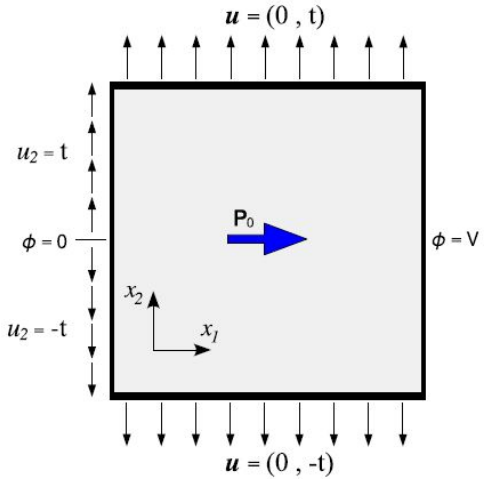


Normalized:

1 - Dimension: 200x200.

2 - $P_0$ = [1,0]

3 - $u_2$ = ±t. (crack)

4 - dV=V.

5 - **h≃1. (80 000 tri)**

6 - D·n=0 on the boundary surfaces. ($\varepsilon_0$<<1)

7 - d(p+/-)/dn=0 in all BC and interface.

# Numerical simulations

Computational domain and parameter setting

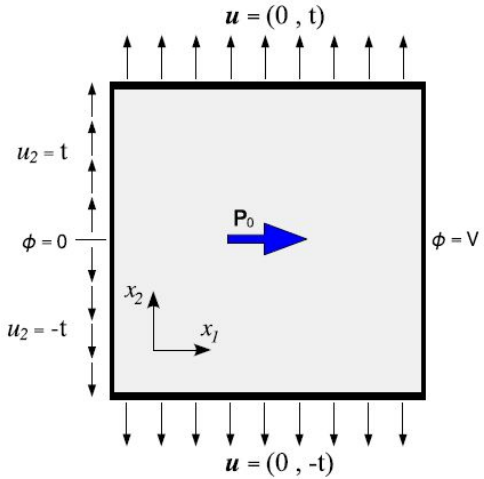


Normalized:

8 - $BaTiO_3$

9 - $K_c$=0.49 MPa$\sqrt{m}$. (intrinsic fracture toughnes, Curie Temp. / paraelectric / no domain switching )

10 - E=100GPa, $\nu$=0.37, $G_c$=2J/$m^2$,$G'_c$=4

11 - **$\kappa$=2. (h/$\kappa$=0.5, h\$\kappa$<<1**[29,30]**,**

h/$\kappa$=1 is ok, but free surface over estimation).

12 - $a_0'$=0.1 (Sharp domain wall).

# Numerical simulations

Computational domain and parameter setting

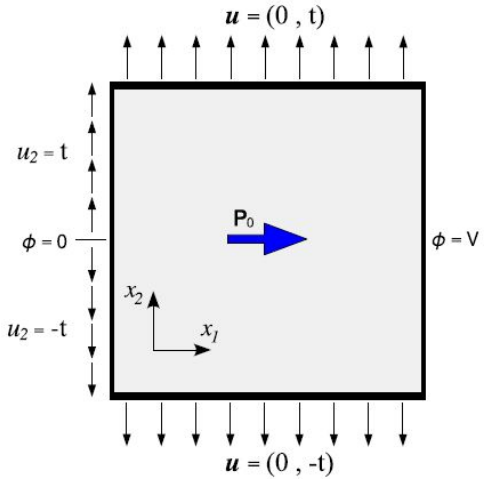


Normalized:

13 - $\delta_{ferro}=\delta_{field}=1\text{-}e3$

14 - $\alpha=2e\text{-}2$

15 - $\mu_p=1$

16 - $\mu_v=15$

17 - $n=100$

18 - $T=3,\ t'_m=0.1$

# Numerical simulations

Mechanical Loading

- V=0 .
  - Permeable $\phi^+ = \phi^-$ and $\mathbf{D}^+ \cdot \boldsymbol{n}^+ = \mathbf{D}^- \cdot \boldsymbol{n}^-$
  - Impermeable. $\mathbf{D}^+ \cdot \boldsymbol{n}^+ = \mathbf{D}^- \cdot \boldsymbol{n}^- = 0$

# Numerical simulations

Permeable crack

- t=0.9
- v<0.02

a) Crack appears.

b) P=[1,0]->[0,1] near the crack.

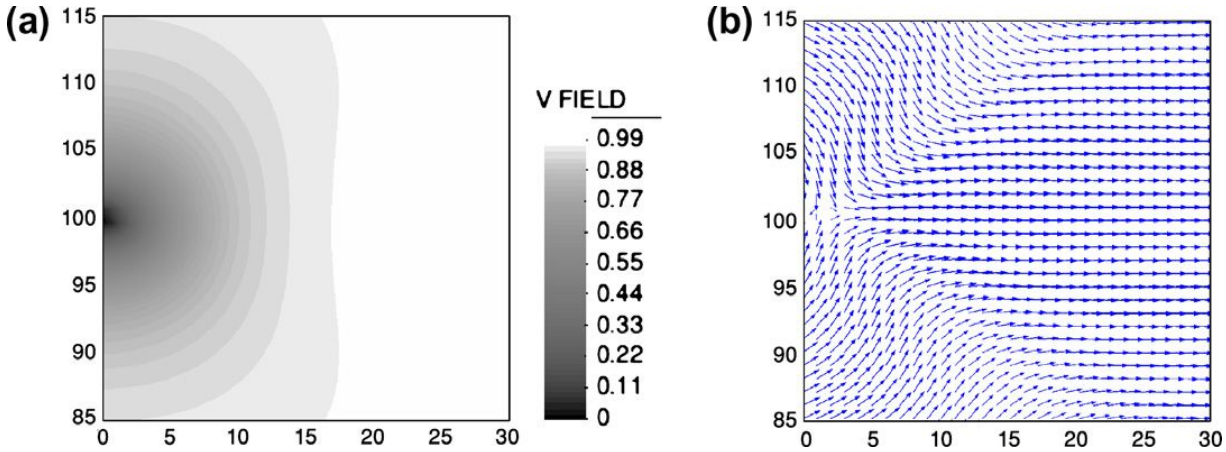

# Numerical simulations

Permeable crack

a) t = 1.05
b) t = 2.49
c) t = 2.58
d) t = 2.67

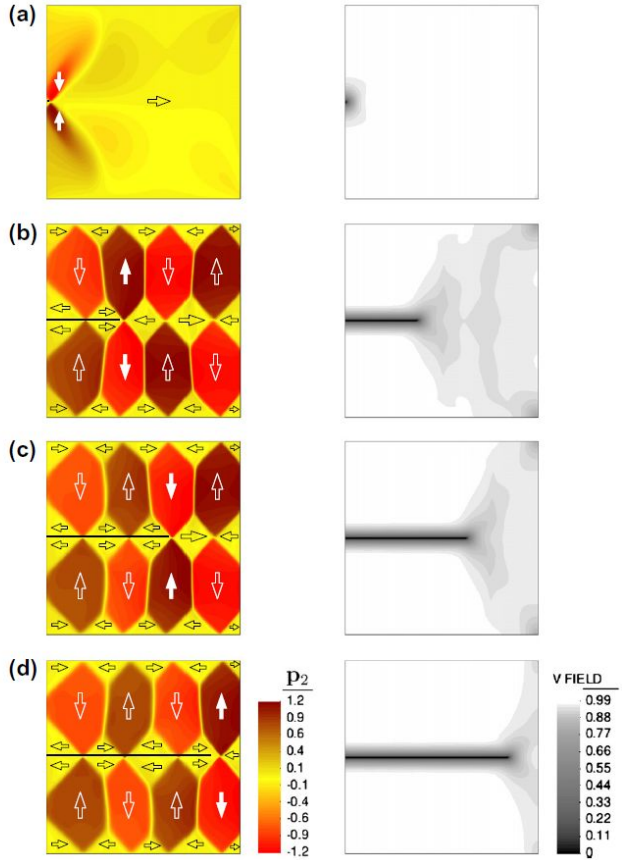

# Numerical simulations

Permeable crack

a) t = 1.05 , n++ -> 2 twins ahead the crack (wing).

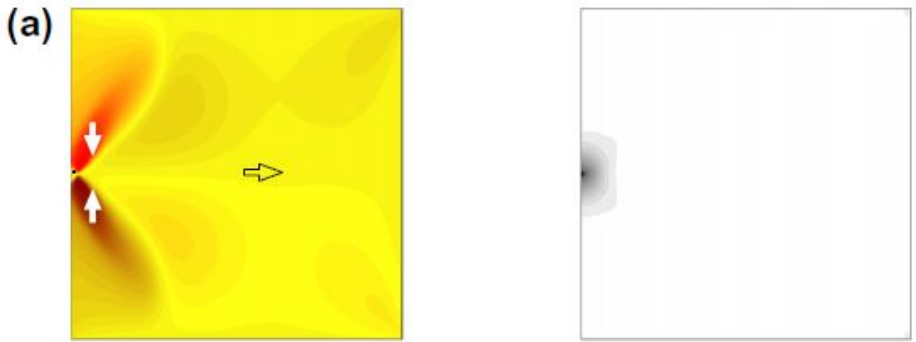

# Numerical simulations

Permeable crack

b) t = 1.05 , More Twins. Due to initial twins touching outter boundary (D·n=0)[49].

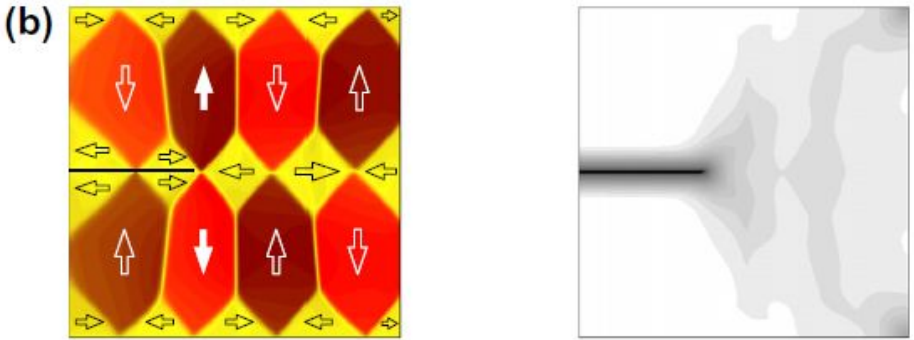

# Numerical simulations

Permeable crack

c) t = 2.58
d) t = 2.67

Crack propagation.

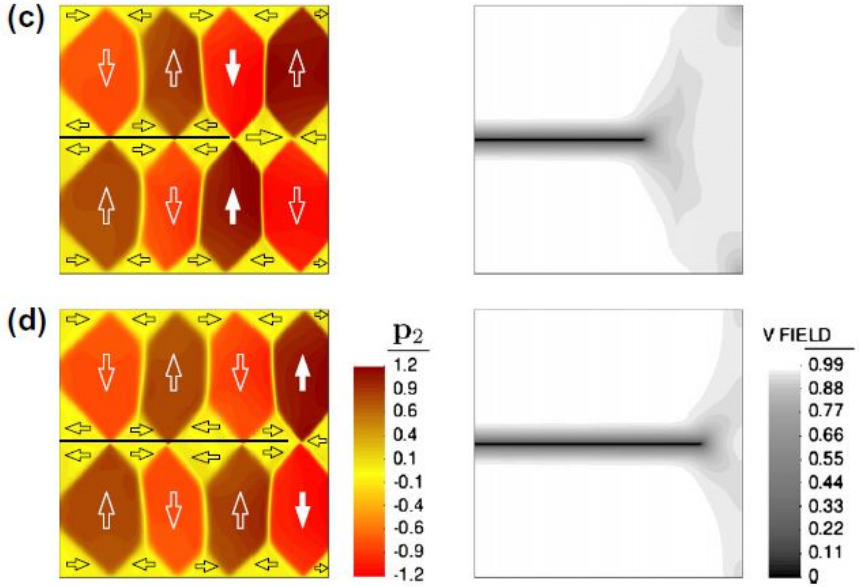

# Numerical simulations

Permeable crack

1) Single-Phase (no twin)
2) Multiphase (Perm)
3) Multiphase(ImPerm)

All: crack initiation around 0.9

Single > Perm > ImPerm

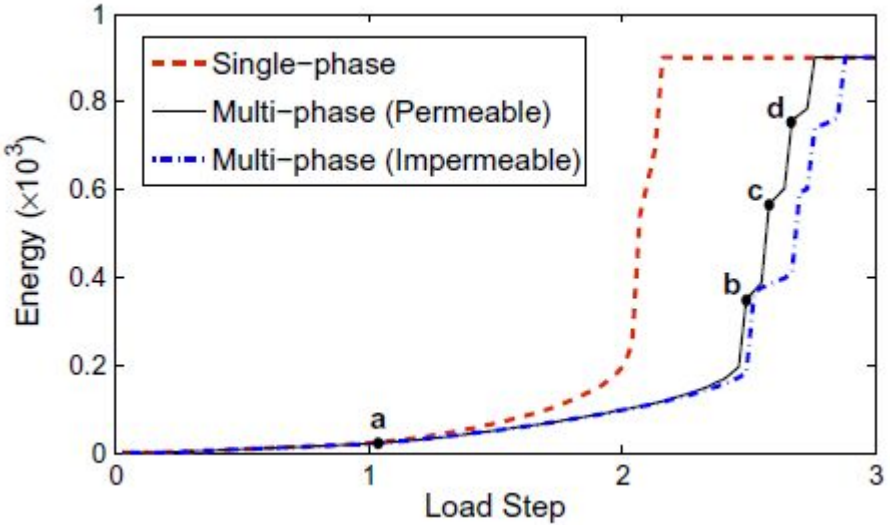

# Numerical simulations

Permeable crack

a) Crack formation.

b), c), d) $\sigma_{22}$ countered, abruptly cracks.[45,49,50]

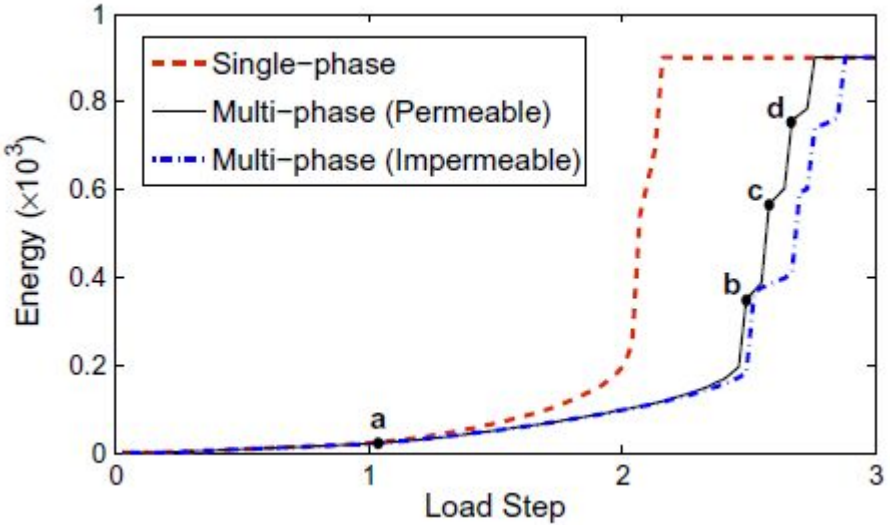

# Numerical simulations

Permeable crack

a) Cross section before the crack, before and ahead the crack.
b) $\sigma_{22}$ increases in the crack region. Twin toughening.

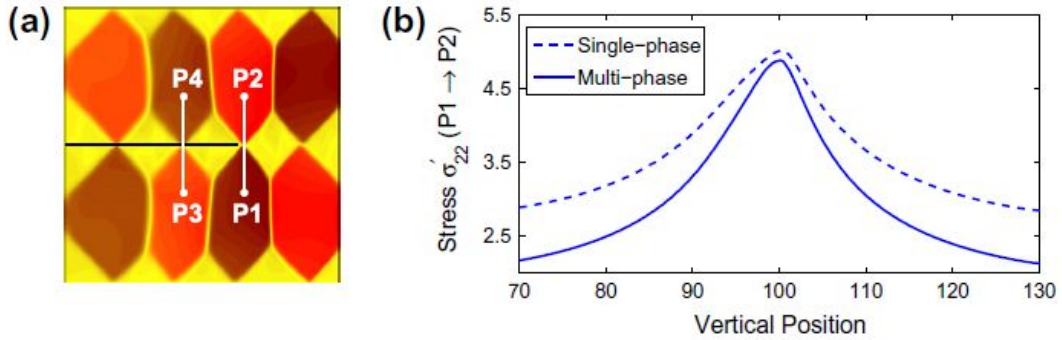

# Numerical simulations

Permeable crack

After crack

1) $\sigma_{22}$ , $\sigma_{12}$ = 0, because traction free BC.
2) $\sigma_{11}$ not 0, near crack edges. (no traction free BC.).

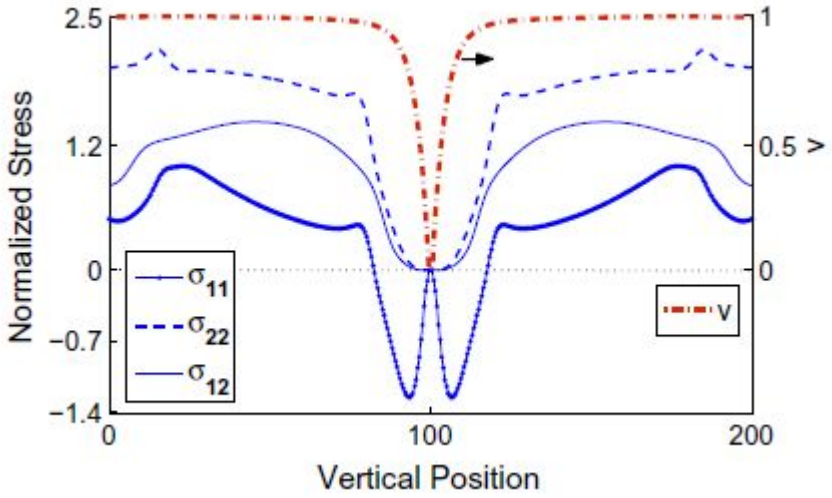

# Numerical simulations

Impermeable crack

Why ImPerm has slower crack propagation rate?

$$\uparrow E \rightarrow \uparrow \sigma_{22} \rightarrow \uparrow h$$

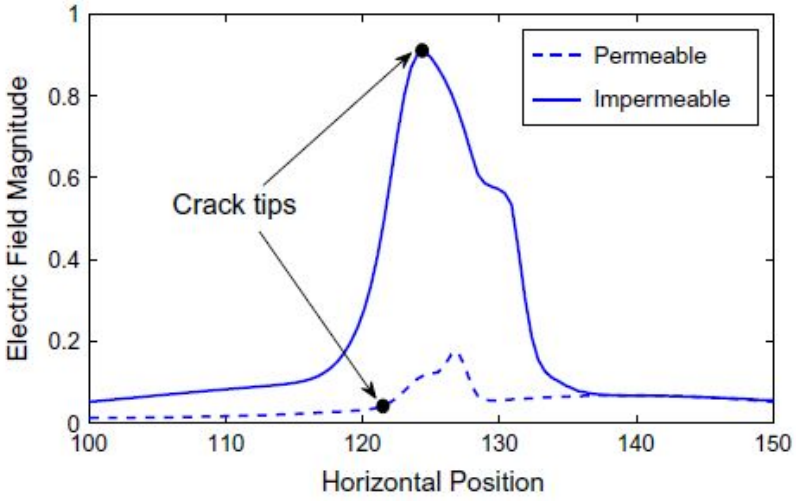

# Numerical simulations

Impermeable crack

Free-polarization BC -> crack $P_2$=0 .

Perm -> $\kappa$≈0-> ImPerm

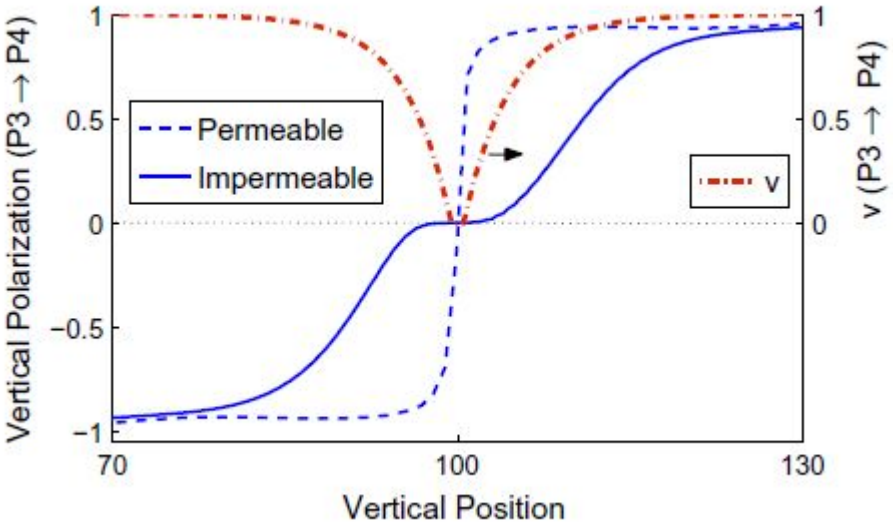

# Numerical simulations

Impermeable crack

Domain walls -> |D|=0.  a) Perm: D·n not 0, no crack.  b)ImPerm: D·n=0, crack + Boundary layer.

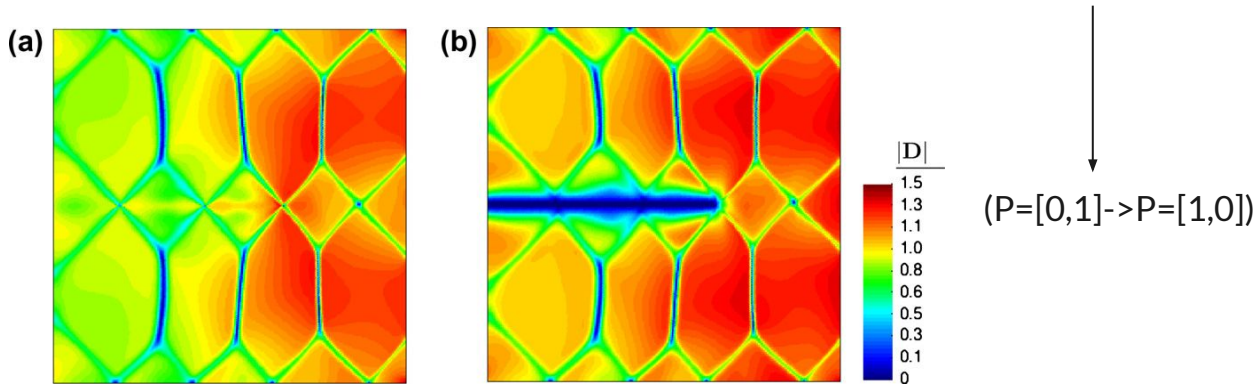

# Numerical simulations

Impermeable crack

$D_1$=0 inside the domain and not to 0 in the crack edge and boundaries.

$D_2$=0 in the crack edge and boundaries and not 0 inside the domain.

This shows the Boundary layer in the edge of the crack ($D_1$ not =0).

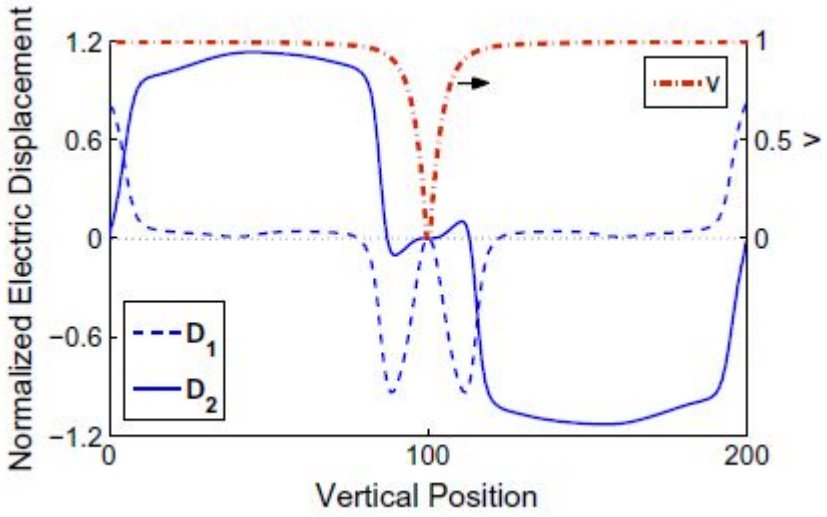

# Numerical simulations

Electromechanical loading

E=-V/L.

More complex -> E -> twin and P.

↑V -> coercive stress, shrinked/disipated twins ahead the crack.

# Numerical simulations

Electromechanical loading

Permeable:

a) E=1e-3
b) E=1e-4

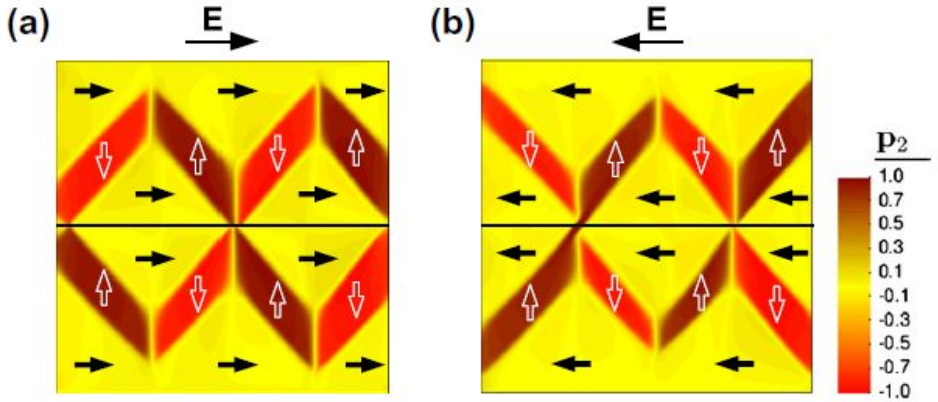

# Numerical simulations

Electromechanical loading

a) ↑V -> Single-phase is recovered.
b) Small -V -> not consistent twins and toughening. ↑-V -> Single-phase recovery.

*Permeable

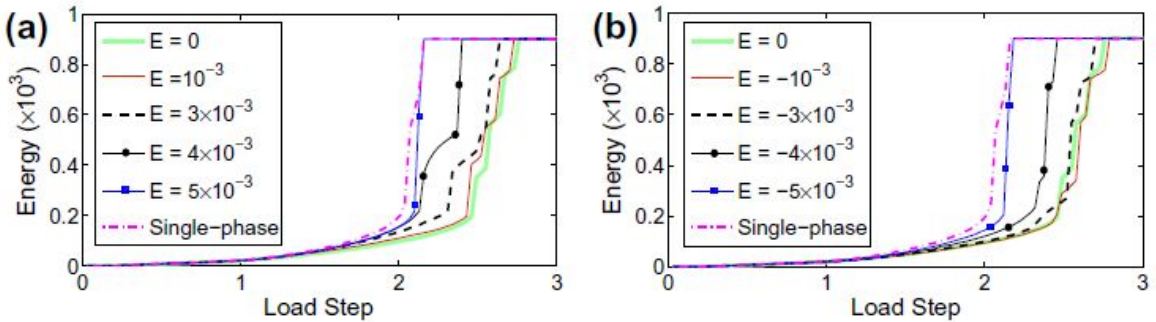

# Numerical simulations

Electromechanical loading

a) Small V -> not consistent twins and toughening. ↑ V -> Single-phase recovery.
b) Small -V -> not consistent twins and toughening. ↑-V -> Single-phase recovery.

*Impermeable

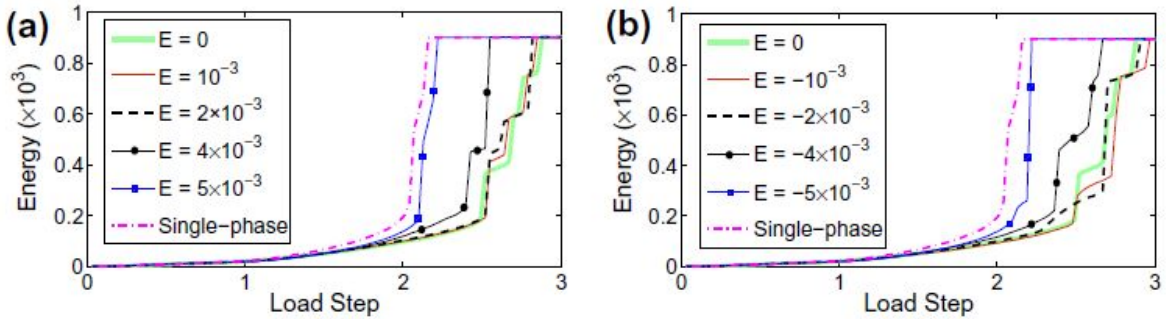

# Conclusions

Reproduction of:

1) Slow-fast crack propagation.
2) Retarding effect (Impermeable).
3) Low applied electric fields below coercive field[52,55].
4) High applied electric fields with coercive magnitude[56].

# Conclusions

Pro: Major technological implementations.

Future research:

1) Anisotropy[49].
2) More realistic BC.
3) Selection of $\mu_p$ and $\mu_v$.

# Review

How Elastic  potential is addressed?

$$E_\kappa[\boldsymbol{u}, v] = \int_\Omega (v^2 + \eta_\kappa) F(\boldsymbol{\varepsilon}(\boldsymbol{u}))\, \mathrm{d}\Omega + G_c \int_\Omega \left[ \frac{(1-v)^2}{4\kappa} + \kappa |\nabla v|^2 \right] \mathrm{d}\Omega - \int_{\Gamma_{N,\boldsymbol{u}}} \boldsymbol{t} \cdot \boldsymbol{u}\, \mathrm{d}S$$

?

$$H[\boldsymbol{u}, v, \mathbf{p}, \phi] = \int_\Omega h(\boldsymbol{\varepsilon}(\boldsymbol{u}), \mathbf{p}, \nabla \mathbf{p}, \mathbf{E}(\phi), v)\, \mathrm{d}\Omega + G_c \int_\Omega \left[ \frac{(1-v)^2}{4\kappa} + \kappa |\nabla v|^2 \right] \mathrm{d}\Omega - \int_{\Gamma_{N,\boldsymbol{u}}} \boldsymbol{t} \cdot \boldsymbol{u}\, \mathrm{d}S + \int_{\Gamma_{N,\phi}} \omega \phi\, \mathrm{d}S$$

# References


[1] Zhang TY, Gao CF. Theor Appl Fract Mech 2004;41:339.

[2] Schneider GA. Annu Rev Mater Res 2007;37:491.

[3] Kuna M. Eng Fract Mech 2010;77:309.

[4] Han XL, Li XJ, Mao SX. Metall Mater Trans A 2002;33:2835.

[5] Rajapakse RKND, Zeng X. Acta Mater 2001;49:877.

[6] Beom HG, Atluri SN. J Mech Phys Solids 2003;51:1107.

[7] Sheng JS, Landis CM. Int J Fract 2007;143:161.

[8] Hackemann S, Pfeiffer W. J Eur Ceram Soc 2003;23:141.

[9] McMeeking RM, Landis CM. Int J Eng Sci 2002;40:1553.

[10] Wang JX, Landis CM. J Mech Mater Struct 2006;1:1075.

[11] Hwang SC, Lynch CS, McMeeking RM. Acta Mater 1995;43:2073.

[12] Zhu T, Yang W. Acta Mater 1997;45:4695.

[13] Yang W, Zhu T. J Mech Phys Solids 1998;46:291.

[14] Zhu T, Yang W. J Mech Phys Solids 1999;47:81.

# References


[16] Schrade D, Mueller R, Xu B, Gross D. Comput Methods Appl MechEng 2007;196:4365.

[17] Xu BX, Schrade D, Mueller R, Gross D. Comput Mater Sci 2009;45:832.

[18] Su Y, Landis CM. J Mech Phys Solids 2007;55:280.

[19] Dayal K, Bhattacharya K. Acta Mater 2007;55:1907.

[20] DeSimone A. J Intell Mater Syst Struct 1994;5:787.

[21] DeSimone A. Z Angew Math Mech 1996;76:397.

[22] Wang J, Zhang TY. Acta Mater 2007;55:2465.

[23] Song YC, Soh AK, Ni Y. J Phys D: Appl Phys 2007;40:1175.

[24] Arias I, Serebrinsky S, Ortiz M. Acta Mater 2006;54:975.

[25] Gao HJ, Zhang TY, Tong P. J Mech Phys Solids 1997;45:491.

[26] Francfort GA, Marigo JJ. J Mech Phys Solids 1998;46:1319.

[27] Bourdin B, Francfort GA, Marigo JJ. J Mech Phys Solids 2000;48:797.

[28] Bourdin B. Interfaces Free Bound 2007;9:411.

[29] Bourdin B, Francfort GA, Marigo JJ. J Elast 2008;91:5.

# References


[30] Amor H, Marigo JJ, Maurini C. J Mech Phys Solids 2009;57:1209.

[31] Xu XP, Needleman A. J Mech Phys Solids 1994;42:1397.

[32] Camacho GT, Ortiz M. Int J Solids Struct 1996;33:2899.

[33] Moes N, Dolbow J, Belytschko T. Int J Numer Methods Eng 1999;46:131.

[34] Oliver J, Huespe AE, Pulido MDG, Chaves E. Eng Fract Mech2002;69:113.

[35] Li JY. Mech Mater 2009;41:1125..

[36] Devonshire AF. Philos Mag 1949;40:1040.

[37] Devonshire AF. Philos Mag 1951;42:1065.

[38] Li YL, Cross LE, Chen LQ. J Appl Phys 2005;98:064101.

[39] Wang YL, Tagantsev AK, Damjanovic D, Setter N, Yarmarkin VK, Sokolov AI, et al. J Appl Phys 2007;101:104115.

[40] Griffith AA. Philos Trans Royal Soc London 1921;Series A-221:163.

[41] Abdollahi A, Arias I, in preparation.

[42] Parton VZ. Acta Astronaut 1976;3:671.

# References


[43] Vendik OG, Zubko SP. J Appl Phys 2000;88:5343.

[44] Deeg WFJ. PhD thesis, Stanford University; 1980.

[45] Meschke F, Raddatz O, Kolleck A, Schneider GA. J Am Ceram Soc2000;83:353.

[46] Stemmer S, Streiffer SK, Ernst F, Ruhle M. Philos Mag A1995;71:713.

[47] Floquet N, Valot CM, Mesnier MT, Niepce JC, Normand L, ThorelA, et al. J Phys III 1997;7:1105.

[48] Dadvand P, Rossi R, Onate E. Arch Comput Methods Eng 2010;17:253.

[49] Fang DN, Jiang YJ, Li S, Sun CT. Acta Mater 2007;55:5758.

[50] Meschke F, Kolleck A, Schneider GA. J Eur Ceram Soc 1997;17:1143.

[51] Ricoeur A, Kuna M. J Eur Ceram Soc 2003;23:1313.

[52] Sun CT, Park SB. Ferroelectrics 2000;248:79.

[53] Li WY, McMeeking RM, Landis CM. Eur J Mech A – Solids2008;27:285.

[54] McMeeking RM. Eng Fract Mech 1999;64:217.

[55] Tobin AG, Pak YE. Proc SPIE, Smart Struct Mater 1993;1916:78.

[56] Schneider GA, Heyer V. J Eur Ceram Soc 1999;19:1299.